

Research Article

Risk Propagation Model and Simulation of Schedule Change in Construction Projects: A Complex Network Approach

Yusi Cheng , Jingfeng Yuan , Lei Zhu , and Wei Li 

School of Civil Engineering, Southeast University, Nanjing 210096, China

Correspondence should be addressed to Jingfeng Yuan; 101011337@seu.edu.cn

Received 17 September 2020; Revised 4 October 2020; Accepted 13 October 2020; Published 7 December 2020

Academic Editor: Guangdong Wu

Copyright © 2020 Yusi Cheng et al. This is an open access article distributed under the Creative Commons Attribution License, which permits unrestricted use, distribution, and reproduction in any medium, provided the original work is properly cited.

Construction schedules play an important role in construction project management. However, during construction activities, risks may arise due to unexpected schedule changes, resulting in the ineffective delivery of projects. This study aims to reveal the law of schedule change risk propagation and to analyze the effects on the risk propagation through numerical simulations. First, construction projects are represented by activity-on-node (AON) networks. A model of risk propagation is then built based on a susceptible-infected (SI) model considering the effects of the nodal characteristics on the propagation process. Next, the model is tested on a real-world project to examine cascading failures with varying parameters. The experimental results demonstrate that the model is effective in identifying the activities most capable of affecting a project schedule and evaluating the impact of schedule change risk propagation. This study will provide a basis for enhancing the robustness of AON networks and controlling the propagation of schedule change risks.

1. Introduction

A construction project is an organized process of constructing a building or structure under time, cost, and quality constraints [1]. Considering the complexity and the uniqueness of each project, planning and scheduling have become vital procedures in construction project management [2]. However, schedules are frequently changed in construction projects. These changes may be caused by owners, contractors, consultants, designers, or the environment [3, 4]. A schedule change often leads to a decline in worker's productivity and an increase in the probability of cost overruns and completion delays [5, 6].

Project managers use a schedule to help plan, execute, and control project activities [7]. Currently, most scheduling tools use the activity-on-node (AON) representation and the critical path method (CPM) [8]. AON denotes activities and the dependencies between activities as nodes and arrows, respectively. Based on an AON network, the CPM explores the critical activities and provides activity float times, which allows continuous monitoring of the schedule and provides alerts of the possibility of project delays. Unfortunately,

construction projects are affected by risks, almost all of which are directly or indirectly related to the schedule of activities [2, 9]. As a result, the start times and durations of activities in an AON network are no longer deterministic, and identification of the critical path may be imprecise. Furthermore, due to complex logical dependencies between activities in an AON network, a schedule change of one activity may affect its succeeding activities [10]. This can cause issues such as disorganized planned resources [11], increased communication costs, and misunderstandings [12], which initiates change risk propagation throughout an AON network [8, 13]. Therefore, it is essential to explore the mechanism of risk propagation of schedule changes.

In recent years, several studies have examined the modeling of construction schedule risks. Previous studies mainly focused on identification and evaluation of schedule risks [2–4, 9, 14], simulation of schedule risks in construction projects [10, 13, 15], and analysis of schedule risks with activity sensitivity information [16–18], but less attention has been paid to the topologies of AON networks and predicting the behavior of risk propagation from an overall perspective [8]. Managing risk propagation is a

challenging task across numerous fields, ranging from finance [19], infrastructure management [20], and project management [8, 21–23]. Despite the contextual differences of these domains, complex networks have been successfully applied to modeling the process of sequential risk propagation throughout the network and analyzing the impact of the parameters and characteristics on the merits of risk propagation. In particular, simulation methods based on spreading theories and complex networks have enabled researchers to design more realistic models that take into account nodal characteristics [24]. However, in the previous studies, little work was done to explore the capacities of AON networks to sustain systemic risks caused by schedule changes. To address this research gap, a model based on AON networks must be designed to simulate the risk propagation of schedule changes. The novelty of this study is that schedule change management was investigated from the perspective of systemic risk.

In the context of risk propagation and schedule changes in construction projects, this paper attempts to resolve two issues: (1) how to generate the risk propagation model of schedule changes on the AON network while taking into consideration activity characteristics and the structure of the AON network; and (2) how to assess the capacity of each activity to trigger a catastrophe of schedule changes around the AON network and increase the resilience of the AON network.

To resolve these issues, first, an AON network was abstracted as a directed graph, and the nodal characteristics related to schedule change risks were analyzed. Second, in reference to the susceptible-infected (SI) model, a new risk propagation model for schedule changes was built, which is applicable to directed graphs where a threshold value representing the risk resistance capacity is assigned to each node. Finally, the developed model was tested on an empirical dataset using a numerical simulation to assess the influencing factors and identify the critical activities that have a significant impact. The aim of this paper is to explore the law of schedule change risk propagation and help construction project managers to control risk propagation. Overall, this paper provides a framework for simulating risk propagation and is a valuable addition to project risk management studies.

There are two contributions of this work. First, the classical SI model is adapted for the risk propagation of schedule changes by considering more realistic assumptions, such as directed graphs and the capacity to resist risk. Second, this work allows us to better understand systemic risk in the case of schedule change risk propagation and predict the systemic risks using numerical simulations.

The rest of the paper is organized as follows: Section 2 reviews the related work. In Section 3, a directed graph is defined with key characteristics, after which the improved model and its ability to simulate the process of change risk propagation are discussed. Section 4 presents the initial configuration of the simulation and the subsequent results of the analysis. The conclusions and directions for future research are given in Section 5.

2. Literature Review

2.1. Schedule Change and Risk. In a construction project, a change refers to “any event that results in a modification of the original scope, execution time, cost, and/or quality of work” [25]. Many researchers have studied construction change management, including schedule changes. Love et al. [26] proposed a framework of a system dynamics (SD) model to explore the relationship and consequences of a change. Park and Peña-Mora [27] considered unintended and managerial changes, both of which were represented as iteration loops in the SD model of the project process. Furthermore, the impact of change on project performance was analyzed based on the discovery status and time. Based on Park’s work, Ansari [28] compared alternative change management policies, including funding, outsourcing activities, schedule adjustments, and labor control by taking into account the time, cost, quality, resources, and financial indicators. An extensive review on schedule changes using the SD model can be found in a previous publication [29]. However, in the SD model, upstream changes are immediately accommodated by changing downstream tasks through feedback loops, without considering a chain reaction of changes. Moreover, because tasks are assumed to be uniform in size and fungible within phases, and the dependencies are simplified to functional forms [30], it is difficult to recognize and control changed tasks. Motawa et al. [31] identified the possibility of changes due to project characteristics and cause-and-effect relationships between change causes and corresponding impacts. Zhao et al. [32] represented the information flow between change factors and changes using an activity-based dependency structure matrix and introduced Monte Carlo simulations to analyze the change probabilities of activities. Heravi and Char-khakan [33] subdivided the change implementation phase into change implementation paths and developed a risk index using event tree analysis. However, correlations between the tasks and dynamics of change risk were neglected in these studies. Recent studies of change risk have mainly concentrated on modeling change risk propagation based on complex network models [23], whereas little work has been done in construction change management.

Construction schedules are affected by uncertainties, and schedule risks are inevitable. Recent studies have mainly focused on estimating the project’s overall duration, taking risk factors into consideration. Nasir et al. [14] established a belief network that consisted of activity nodes representing activity duration values and risk nodes describing project conditions, and the network’s output was incorporated into Monte Carlo simulations to evaluate schedule risks. Oliveros and Fayek [34] proposed a fuzzy logic approach to combine the frequency of occurrence and adverse consequences for the attributes of schedule risks and then assessed the relationship between consequences and delay durations. Ökmen and Özta [2] considered the correlation effect between risk factors and activities and captured the correlation by converting qualitative estimates to quantitative values. Luu et al. [3] identified 16 factors of schedule risks and obtained 18 cause-and-effect relationships between these factors through

expert interviews to develop a belief network model. Tokdemir et al. [13] assumed that risks originated from vagueness/uncertainty, task complexity, and vulnerability and defined the labor hour coefficients and the learning rate, both of which determined the activity duration, based on these factors. Cho et al. [35] built a schedule delay estimation model with three fully connected layers: a project attributes layer, a risk factors layer, and a work variation layer. Although the reliability of the duration prediction is crucial for the time performance, previous research ignored the idea that accumulated schedule changes in a complex AON network accounting for unforeseen events being considered as sources of risk. Besides, the impact of the characteristics of AON networks on schedule delays, such as the activity duration, slack time, and node degree, is not considered in these methods. Furthermore, as a result of a chain reaction of changes, a change in one activity's schedule may require changes to successor activities, and a shift to the critical path may be triggered, leading to increased schedule risk [36]. Therefore, in this work, a risk propagation model will be used to extend the concept of schedule risks to include the change risks and the dynamic character of an activity, resulting in a model that is then capable of illustrating the triggering of a catastrophe of schedule changes.

2.2. Risk Propagation Model. Previous studies analyzed the dynamic characteristics of risk propagation across complex systems and proposed three common mathematical models: a load-capacity model [37], an epidemic disease model [38], and a threshold model [39]. In the load-capacity model, a node fails if its load becomes larger than its capacity, and the load is represented as the total number of shortest paths passing through the node. The epidemic model is used to describe the dynamic process of the spread of disease. One of the basic epidemic models is the SI model, which is composed of three components: susceptible nodes, infected nodes, and the infection rate. Together, these components represent the probability of transmitting disease between a susceptible node and an infected node. In addition, the threshold model explains the propagation according to a simple threshold rule. Due to the difficulties in describing the risk of schedule changes as shortest paths, we chose the SI model for our work and modified it by adding a threshold in the propagation process. In fact, the lack of a threshold may make the propagation persist in networks of infinite size [40].

Risk propagation models have widely been applied in various fields, and the core parts of the models are risk metrics and the threshold. Ellinas et al. [8] examined the likelihood of a large-scale catastrophe triggered by a single task failure in an AON network, and the propagation process was measured by the topological, temporal, and quality aspects of the AON network. Furthermore, the Ellinas model was extended to include the role of indirect exposure [21] and the impact of contractor activity [36]. However, for a node in the Ellinas model, its failure risk at a given time step is perceived as the maximum risk, rather than the combined risk, due to its predecessors. Guo et al. [22] proposed a flow

redistribution model to analyze cascade failures in AON networks. In this model, an initial risk load was defined as a function of the node degree determined by the activity duration, and a risk threshold was assumed to be correlated with the initial risk. Chen et al. [41] improved the epidemic model to study risk propagation in an emergency logistics network and evaluated the risk infection and the risk threshold using eigenvector centrality and a material reservation index, respectively. Li et al. [23] studied the risk propagation of design changes in a multilayer network with interacting products and organization layers and determined the risk threshold using the out-degree of the node. Rey [24] built an epidemic-based model to predict the spread of advanced malware with the infection probability based on the number of infectious neighbors. However, these models cannot describe the characteristics of the change risk propagation in AON networks. To the best of our knowledge, there are few risk propagation models used to analyze schedule change risks. In particular, risk metrics and the threshold in the risk propagation model of schedule changes need to be tailored to AON networks and schedule change scenarios.

3. Materials and Methods

To study the risk propagation of schedule changes, an AON network was first introduced, in which nodes represent activities and links represent logical dependencies. Although indicators for network topology are often analyzed, they are not suitable for directly describing the dynamic process of risk propagation in networks. Therefore, a risk propagation model for schedule change risk was then developed based on an epidemic model and a threshold model. Moreover, the impact of activity characteristics and the structure of the AON network are considered in the proposed model, making it more suitable for the study of schedule change risk propagation.

3.1. AON Network of Construction Projects. An AON network is a graphical representation of a project schedule, in which nodes indicate activities and arc arrows (links) show the dependency between two activities. There are four types of dependencies: finish to start (FS), finish to finish (FF), start to start (SS), and start to finish (SF). Dependencies can be affected by time constraints, lags, and leads. According to the Project Management Body of Knowledge (PMBOK) [42], lag is defined as "the amount of time whereby a successor activity will be delayed with respect to a predecessor activity," while a lead is "the amount of time whereby a successor activity can be advanced with respect to a predecessor activity." Once the network has been developed, each activity node also has a start date and a finish date. To better understand an AON network, an example with six activities is considered, as shown in Figure 1. Using i , j , and k in the network as an example, the immediate predecessor of activities j and k is activity i . "FS + 2" between i and j means that before j can start, it must wait at least two days after the completion of i . "SS" between i and k means that k cannot start unless i has been initiated.

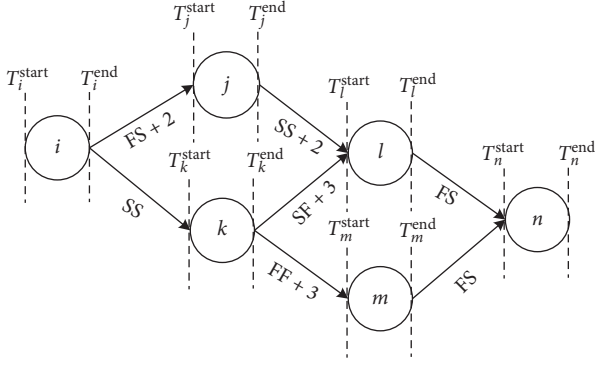


FIGURE 1: AON network abstraction.

Based on the AON network, the project schedule is represented by a directed graph $G = (V, E)$, where $V = \{v_1, v_2, \dots, v_n\}$ is the node set and $E \subseteq V \times V$ is the edge set. The adjacency matrix $A = (a_{ij})_{n \times n}$ is defined, where $a_{ij} = 1$ if $(v_i, v_j) \in E$ and $a_{ij} = 0$ if $(v_i, v_j) \notin E$. A node v_i is a predecessor of a node v_j if $a_{ij} = 1$, and, equivalently, v_j is a successor of v_i . The set of predecessors of v_i is referred to as N_i^- , and the set of successors of v_i is referred to as N_i^+ . The start and end dates of node v_i are denoted as T_i^{start} and T_i^{end} , respectively. The dependency and the time constraint of edge e_{ij} are denoted as $d_{ij} \in \{\text{FS}, \text{FF}, \text{SS}, \text{SF}\}$ and $t_{ij} \in \mathbb{R}$, respectively. $t_{ij} \geq 0$ if there is lag between v_i and v_j , and $t_{ij} < 0$ if there is lead time between v_i and v_j . It is worth noting that an AON network captures both global information (i.e., topological features) and local information (i.e., activity duration, time between consecutive activities and time constraints) [8]. These pieces of information play an important role when the schedule changes. Therefore, we consider a mechanism based on all of this useful information.

3.2. Risk Propagation Model for Schedule Change. Schedule change risk refers to the possibility of loss caused by the inability to execute the original schedule. The dependency relationships between activities in the AON network, such as causal relationships and resource constraints, are considered as a way to diffuse the change risk. When the change risks of nodes surpass their capacities, these nodes will trigger the potential change risk of successors. Specifically, the risk propagation of a schedule change in this paper describes the occurrence of a schedule change of one activity and the propagation of the change risk through the AON network until the number of infected activities is no longer significantly increased.

3.2.1. Assumptions. Considering the properties of the schedule change risk, the following assumptions are proposed to build the model:

- (1) Nodes in the network can only be directly infected by their predecessors because the dependency between two activities is directed
- (2) Nodes have four possible states: susceptible (S), start date infected (S-I), end date infected (E-I), and simultaneous S-I and E-I ((S-I, E-I))

A susceptible node is transformed to an infected state when its change risk exceeds its capacity. Once a node is infected, its state will never change again. To focus on predicting the behavior of the change risk propagation and evaluating the factors affecting risk propagation, the recovered state and transformation from infected to susceptible are not considered in this paper. Moreover, the schedule change of a node can be divided into two types: start date change and end date change, which correspond to S-I and E-I, respectively.

- (3) The AON network is static in the model, which indicates that the structure does not change.

In fact, the AON network is constantly adjusted. Nodes are deleted, added, and delayed as a result of events, such as a change order from the owners, a changing environment, and ineffective communication. To reduce the complexity of the model and highlight the impact of risk propagation, we assume that the network structure does not change.

- (4) The model is discrete, but the nodes are not infected in the project time order.

There are two types of times in the model: project time and simulation time. The start and end dates of each node are the project time. The simulation time represents the steps of propagation, and a node can be affected by its predecessors at each step. Sometimes, these two types of times are contradictory. For example, in Figure 2, all the nodes are assumed to be infected. i is the initial node infected at simulation time t_0 . m and l are both infected at simulation time t_2 , while m starts after l ends in the project time. Rather than precisely simulating the execution of a schedule under a change risk, this paper focuses on measuring the AON performance when faced with disruptions. As a result, the simulation time is used during the process of risk propagation.

- (5) Before the schedule changes occur ($t < 0$), all the nodes are S nodes. A schedule change then occurs on one node at $t = 0$.

3.2.2. Model Dynamics. The propagation of a schedule change in an AON network is related to the type of schedule change and the dependencies of subsequent nodes. The schedule change is divided into an end date change and a start date change based on the impact of schedule changes on activities. Figure 3 shows the successive infection process of a schedule change risk. It is assumed that the risk of an end date change on node i 's predecessor i^- has occurred, and four kinds of dependencies between i^- and i are considered. (1) In Figure 3(a), if the dependency is FS, then the end date change of i^- may trigger the risk of a start date change and an end date change on i at the same time. (2) If the dependency is SS, then the possibility of affecting i 's schedule is very low. (3) If the dependency is FF, then an end date change of i^- may trigger the risk of end date changes on i . (4) If the dependency is SF, then the possibility of affecting i 's

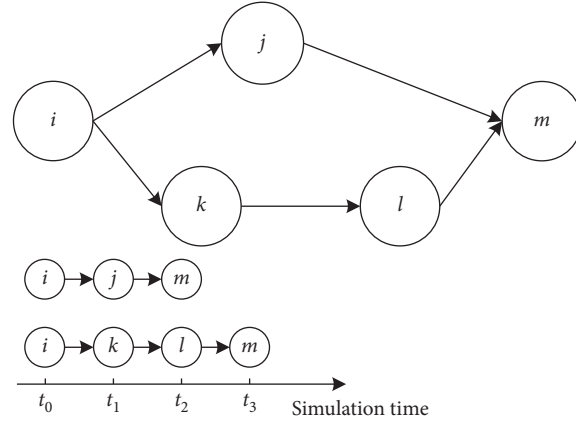
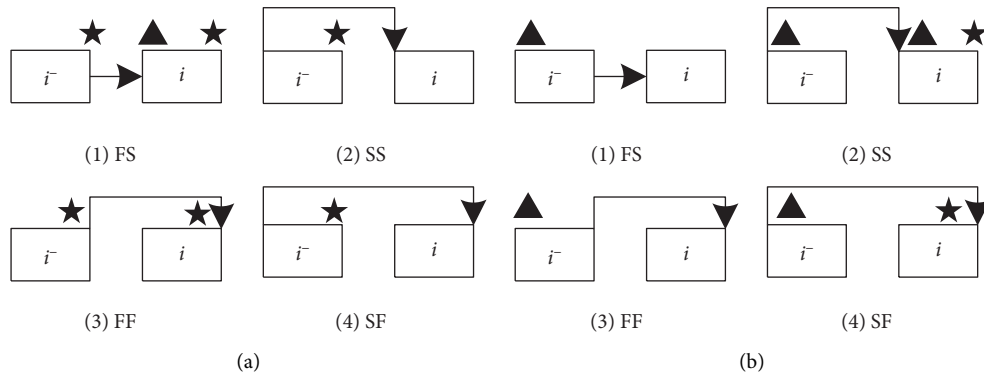


FIGURE 2: Project time and simulation time.

FIGURE 3: Infection of schedule change risk. \star represents an end date change risk, and \blacktriangle represents a start date change risk. Node i^- is the predecessor of node i . Risk propagation caused by (a) the end date change and (b) start date change.

schedule is very low. Considering a start date change, similar cases can be concluded and are shown in Figure 3(b).

3.2.3. Risk Threshold and Infection Rate for Risk of End Date Change. The node's risk threshold reflects the ability of the activity to resist the schedule change risk, and the threshold is limited due to the cost. As shown in Figure 3, node i 's end date change risk may be triggered in four situations: end date change of $i^- + FS$, end date change of $i^- + FF$, start date change of $i^- + SS$, and start date change of $i^- + SF$.

(1) *Situation a: End Date Change of $i^- + FS$.* In this case, two indicators of the risk threshold are considered. First, if the activity duration is long, the activity's capacity to resist changes of the end date will be high. That is because change disruptions are more likely to be absorbed by a longer duration. Let D_i be the duration of node i , and $f^D: R^+ \rightarrow [0, 1]$ be a normalization function that normalizes the duration between 0 and 1. The duration aspect of the end date threshold of node i , C_i^D , can be set as follows:

$$C_i^D = f^D(T_i^{\text{end}} - T_i^{\text{start}}) = f^D(D_i). \quad (1)$$

Second, as nodes with greater out-degrees have higher impacts on their successors [23], more resources are allocated

to these nodes to prevent change risks, which indicates a higher risk threshold. Based on the analysis above, the end date threshold of node i , $C_i^{\text{END-TH}}$, is expressed as follows:

$$C_i^{\text{END-TH}} = \alpha (f^O(K_{i(\text{out})}))^{\beta_K} (C_i^D)^{\beta_D}, \quad (2)$$

where $\alpha > 0$, $\beta_K > 0$, and $\beta_D > 0$ are adjustable parameters. α is correlated with the cost invested into activities and is defined as the capacity level. $K_{i(\text{out})}$ represents the out-degree of node i . f^O is the normalization function of the out-degrees. β_K and β_D reflect the influence of the out-degree and the duration on the risk capacity, respectively.

With respect to the infection rate, the network structure and slack time between subsequent nodes affect the way in which the propagation process unravels. Eigenvector centrality measures a node's influence on a network based on the concept that a node pointing to well-connected nodes has high eigenvector centrality. As eigenvector centrality is a good measure of the spreading power [43], it is used to evaluate the infection rate. The structural aspect of infection rate from node i^- to i is expressed as follows:

$$I_{i^- \rightarrow i}^S = f^E(C_{i^-}^E), \quad (3)$$

where $C_{i^-}^E$ is the eigenvector centrality of node i^- and f^E is the normalization function of the eigenvector centralities.

The slack time between node i and its predecessor i^- is the amount remaining after the time constraint is deducted from the time difference $\|T_i^{\text{start}} - T_{i^-}^{\text{end}}\| - t_{i^-}$. The infection rate decreases as the slack time increases, as there is more time to react before i starts [8]. Therefore, the infection rate from i^- to i is equal to

$$I_{i^- \rightarrow i}^{\text{END-R}} = \gamma (I_{i^- \rightarrow i}^S)^{\beta_E} \left(f^S \left(\|T_i^{\text{start}} - T_{i^-}^{\text{end}}\| - t_{i^-} \right) \right)^{-\beta_S}, \quad (4)$$

where $\gamma > 0$ is an adjustable parameter, defined as the infection intensity, and f^S is the normalization function of slack time. $\beta_E > 0$ and $\beta_S > 0$ reflect influence of the eigenvector centrality and slack time on the infection rate, respectively.

(2) *Situation b.* End date change of $i^- + \text{FF}$. In this situation, the end date of i is directly dependent on the end date of i^- . Consequently, the duration of i cannot mitigate changes of i^- . Except for this, a similar expression to equation (2) for $C_i^{\text{END-TH}}$ can be obtained:

$$C_i^{\text{END-TH}} = \alpha (f^O(K_{i(\text{out})}))^{\beta_K} (f^D(1))^{\beta_D}, \quad (5)$$

where $C_i^{\text{END-TH}}$ in equation (2) is replaced by its minimum value $f^D(1)$. A similar approach for calculating the infection rate to that in Situation a is used, in which the slack time is replaced as follows:

$$I_{i^- \rightarrow i}^{\text{END-R}} = \gamma (I_{i^- \rightarrow i}^S)^{\beta_E} \left(f^S \left(\|T_i^{\text{end}} - T_{i^-}^{\text{end}}\| - t_{i^-} - |D_i|\right) \right)^{-\beta_S}. \quad (6)$$

(3) *Situation c.* Start date change of $i^- + \text{SS}$. $C_i^{\text{END-TH}}$ is calculated using equation (2). $I_{i^- \rightarrow i}^{\text{END-R}}$ is similar to equation (4), except that the slack time is replaced as follows:

$$I_{i^- \rightarrow i}^{\text{END-R}} = \gamma (I_{i^- \rightarrow i}^S)^{\beta_E} \left(f^S \left(\|T_i^{\text{start}} - T_{i^-}^{\text{start}}\| - t_{i^-} - |D_i|\right) \right)^{-\beta_S}. \quad (7)$$

(4) *Situation d.* Start date change of $i^- + \text{SF}$. $C_i^{\text{END-TH}}$ is calculated using equation (5). $I_{i^- \rightarrow i}^{\text{END-R}}$ is similar to equation (6) except that the slack time is replaced:

$$I_{i^- \rightarrow i}^{\text{END-R}} = \gamma (I_{i^- \rightarrow i}^S)^{\beta_E} \left(f^S \left(\|T_i^{\text{end}} - T_{i^-}^{\text{start}}\| - t_{i^-} - |D_i| - |D_{i^-}|\right) \right)^{-\beta_S}. \quad (8)$$

3.2.4. *Risk Threshold and Infection Rate for Risk of Start Date Change.* The threshold and infection rate for the start date change risk are calculated using indicators similar to those used for end date changes. As shown in Figure 3, node i 's start date change risk may be triggered in two situations: end date change of $i^- + \text{FS}$ and start date change of $i^- + \text{SS}$.

(5) *Situation e.* End date change of $i^- + \text{FS}$. $C_i^{\text{ST-TH}}$ is the start date threshold of node i , and it is determined using equation (5). $I_{i^- \rightarrow i}^{\text{ST-R}}$ is the infection rate from i^- to i , and it is calculated using equation (4).

(6) *Situation f.* Start date change of $i^- + \text{SS}$. $C_i^{\text{ST-TH}}$ has the same value as the one in Situation e, and $I_{i^- \rightarrow i}^{\text{ST-R}}$ is identical to equation (7).

The risk threshold and infection rate in six different situations are summarized in Table 1.

3.2.5. *Transition Rules.* When the number of node i 's predecessors is greater than 1, two risks may be infected on i independently by different risks on different predecessors, and the infection of the risk is conceived as the combined infection from the predecessors. The state of node i at time step t can be expressed as $S_i^m(t)$, where $m \in \{\text{END}, \text{ST}\}$ denotes the risk type. $S_i^m(t) = 0$ means that i is in S under risk m , and $S_i^m(t) = 1$ means that i is in I under risk m . When $m = \text{END}$, transition rules for i about end date change risk can be specified as follows:

$$S_i^{\text{END}}(t) = \begin{cases} 1, & C_i^{\text{END-TH}}[0] < 1 - \prod_{i^- \in N_i^{a^-} \cup N_i^{c^-}} I_{i^- \rightarrow i}^{\text{END-R}} \text{ or } C_i^{\text{END-TH}}[1] < 1 - \prod_{i^- \in N_i^{b^-} \cup N_i^{d^-}} I_{i^- \rightarrow i}^{\text{END-R}}, \\ S_i^{\text{END}}(t-1), & \text{else,} \end{cases} \quad (9)$$

where $C_i^{\text{END-TH}}[0] = \alpha (f^O(K_{i(\text{out})}))^{\beta_K} C_i^D$ and $C_i^{\text{END-TH}}[1] = \alpha (f^O(K_{i(\text{out})}))^{\beta_K} f^D(1)$ represent two possible values of $C_i^{\text{END-TH}}$. $N_i^{x^-}$ ($x \in \{a, b, c, d, e, f\}$) is node i 's predecessor node set, and for each $i^- \in N_i^{x^-}$, i^- and i are in Situation x .

Meanwhile, $I_{i^- \rightarrow i}^{\text{END-R}}$ takes the corresponding value listed in Table 1. However, when $m = \text{ST}$, transition rules for i about the start date change risk can be specified as follows:

$$S_i^{\text{ST}}(t) = \begin{cases} 1, & C_i^{\text{ST-TH}}[0] < 1 - \prod_{i^- \in N_i^{e^-} \cup N_i^{f^-}} I_{i^- \rightarrow i}^{\text{ST-R}}, \\ S_i^{\text{ST}}(t-1), & \text{else,} \end{cases} \quad (10)$$

TABLE 1: Risk threshold and infection rate in six situations.

	Risk threshold	Infection rate
a	$C_i^{\text{END-TH}} = \alpha (f^O(K_{i(\text{out})}))^{\beta_K} (C_i^D)^{\beta_D}$	$I_{i \rightarrow i}^{\text{END-R}} = \gamma (I_{i \rightarrow i}^S)^{\beta_E} (f^S(T_i^{\text{start}} - T_i^{\text{end}} - t_{ii} - 1))^{-\beta_S}$
b	$C_i^{\text{END-TH}} = \alpha (f^O(K_{i(\text{out})}))^{\beta_K} (f^D(1))^{\beta_D}$	$I_{i \rightarrow i}^{\text{END-R}} = \gamma (I_{i \rightarrow i}^S)^{\beta_E} (f^S(T_i^{\text{end}} - T_i^{\text{start}} - t_{ii} - D_i))^{-\beta_S}$
c	$C_i^{\text{END-TH}} = \alpha (f^O(K_{i(\text{out})}))^{\beta_K} (C_i^D)^{\beta_D}$	$I_{i \rightarrow i}^{\text{END-R}} = \gamma (I_{i \rightarrow i}^S)^{\beta_E} (f^S(T_i^{\text{start}} - T_i^{\text{end}} - t_{ii} - D_i))^{-\beta_S}$
d	$C_i^{\text{END-TH}} = \alpha (f^O(K_{i(\text{out})}))^{\beta_K} (f^D(1))^{\beta_D}$	$I_{i \rightarrow i}^{\text{END-R}} = \gamma (I_{i \rightarrow i}^S)^{\beta_E} (f^S(T_i^{\text{end}} - T_i^{\text{start}} - t_{ii} - D_i - D_i))^{-\beta_S}$
e	$C_i^{\text{END-TH}} = \alpha (f^O(K_{i(\text{out})}))^{\beta_K} (f^D(1))^{\beta_D}$	$I_{i \rightarrow i}^{\text{END-R}} = \gamma (I_{i \rightarrow i}^S)^{\beta_E} (f^S(T_i^{\text{start}} - T_i^{\text{end}} - t_{ii} - 1))^{-\beta_S}$
f	$C_i^{\text{END-TH}} = \alpha (f^O(K_{i(\text{out})}))^{\beta_K} (f^D(1))^{\beta_D}$	$I_{i \rightarrow i}^{\text{END-R}} = \gamma (I_{i \rightarrow i}^S)^{\beta_E} (f^S(T_i^{\text{start}} - T_i^{\text{end}} - t_{ii} - D_i))^{-\beta_S}$

where $S_i(t) \in \{0, 1, 2, 3\}$ indicates the state of node i at time step t , where 0, 1, 2, and 3 represent S, E-I, S-I, and (E-I, S-I), respectively. Based on equations (9) and (10), $S_i(t)$ is determined as follows:

$$S_i(t) = \begin{cases} 0, S_i^{\text{END}} = 0 \text{ and } S_i^{\text{ST}} = 0, \\ 1, S_i^{\text{END}} = 1 \text{ and } S_i^{\text{ST}} = 0, \\ 2, S_i^{\text{END}} = 0 \text{ and } S_i^{\text{ST}} = 1, \\ 3, S_i^{\text{END}} = 1 \text{ and } S_i^{\text{ST}} = 1. \end{cases} \quad (11)$$

Two metrics are used to measure the impact of the change risk. One is the infection node density $Z(t)$, which is the ratio of the number of infected nodes to the number of whole network nodes at time step t :

$$Z(t) = \frac{\sum_{i=1}^N (S_i(t) \neq 0)}{N}, \quad (12)$$

where the value is 1 if $S_i(t)$ is not equal to 0 and the value is 0 if $S_i(t)$ is equal to 0. N is the number of whole network nodes. Since the propagation process will come to an end, $Z(t)$ will converge to a stable value Z^* . Z^* is also used as an indicator related to $Z(t)$.

The other metric is the normalized avalanche size CF_N [22]:

$$CF_N = \frac{\sum_{i=1}^N CF_i}{N(N-1)}, \quad (13)$$

where CF_i denotes the number of the infected nodes after the risk occurs on node i at $t = 0$. According to the type of schedule risk, CF_N can be extended to CF_N^{END} and CF_N^{ST} .

4. Results and Discussion

Simulation experiments were conducted to examine the risk propagation for schedule changes in a construction project. The aim of the project was to deliver a high-rise complex in 800 days. The AON network is shown in Figure 4, with 803 nodes and 1388 directed edges. In Figure 4, the node size is dependent on the node degree that is the number of edges adjacent to the node.

The normalization functions used for durations (f^D), out-degrees (f^O), eigenvector centralities (f^E), and slack time (f^S) were related to the distributions of the data, as shown in Figure 5. As these distributions were heavy tailed, and maximum cutoff values were specified so that any value greater than that would be set to the specified maximum

value. As shown in Figure 5, the cutoff values were set as 20, 5, 0.05, and 10 for f^D , f^O , f^E , and f^S , respectively. Min-max normalization was then used to scale the data.

The effectiveness of the propagation model was analyzed for different values of the parameters. The initial values of the parameters chosen from reasonable ranges are listed in Table 2, and the ranges can be achieved from the following experiments. During simulations, the value of every fixed parameter was set to the initial value correspondingly. The simulation was performed using Python and NetworkX.

The relationship between CF_N and γ is presented in Figure 6, where γ was changed from 0.2 to 3 at a step size of 0.2 and α was set to 0.5, 1, 1.5, 2, 2.5, and 3. Figure 6 shows that with an increase in the adjustable parameter γ , the infection rate increased, and CF_N increased gradually. When γ increased to a certain value, CF_N remained at a stable and high value, indicating a limit to the growth of the propagation. This behavior demonstrated the existence of the basic resilience of the resisting schedule change risk and the limited size of the AON network. The convergence rate and the stable value of CF_N are highly correlated with α . For example, CF_N increased more steeply when $\alpha = 0.5$ than when $\alpha = 3$, and the stable value of the former was roughly four times than that of the latter. Hence, robustness of the AON network increased with the increase in α . However, the robustness of the AON network did not improve significantly when $\alpha \geq 2$, indicating a limit of the marginal capacity of the resistance to risk. In this study, the robustness of an AON network refers to the ability of the AON network to withstand the change risk propagation triggered by a small number of changed activities. The ability can be indicated by CF_N and rate of convergence to the stable state.

The effects of parameters β_E , β_K , β_S , and β_D were investigated, and the results are shown in Figure 7. These parameters were changed from 0.1 to 5, and the step length was 0.1. The initial infected node at $t = 0$ was the node with a maximum eigenvector centrality. Figure 7(a) shows that the higher the value of β_E was, the lower the value of Z^* became. Because the eigenvector centrality was normalized between 0 and 1, the infection rate had a negative relationship with β_E . In addition, Z^* decreased rapidly when β_E was around 1. Figure 7(b) shows that Z^* increased with β_K . Due to the negative relationship between the node capacity and β_K , the increase in β_K led to a decrease in the node capacity and an increase in Z^* . Figure 7(c) shows increasing β_S led to a higher Z^* , resulting from the positive relationship between the infection rate and β_S . Figure 7(d) shows that increasing β_D led to a higher Z^* , resulting from the positive

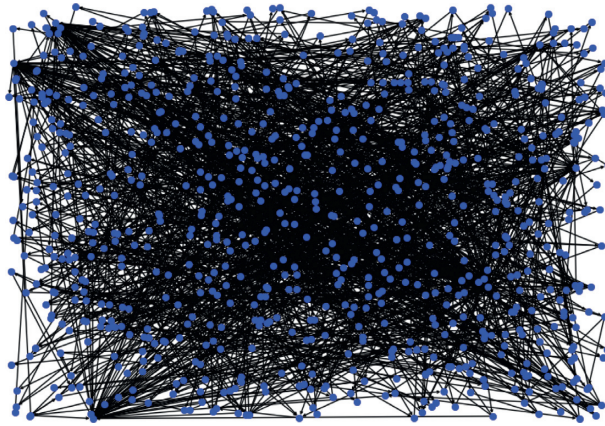


FIGURE 4: An AON network of a construction project with NetworkX random layout. The node size corresponds to the node degree.

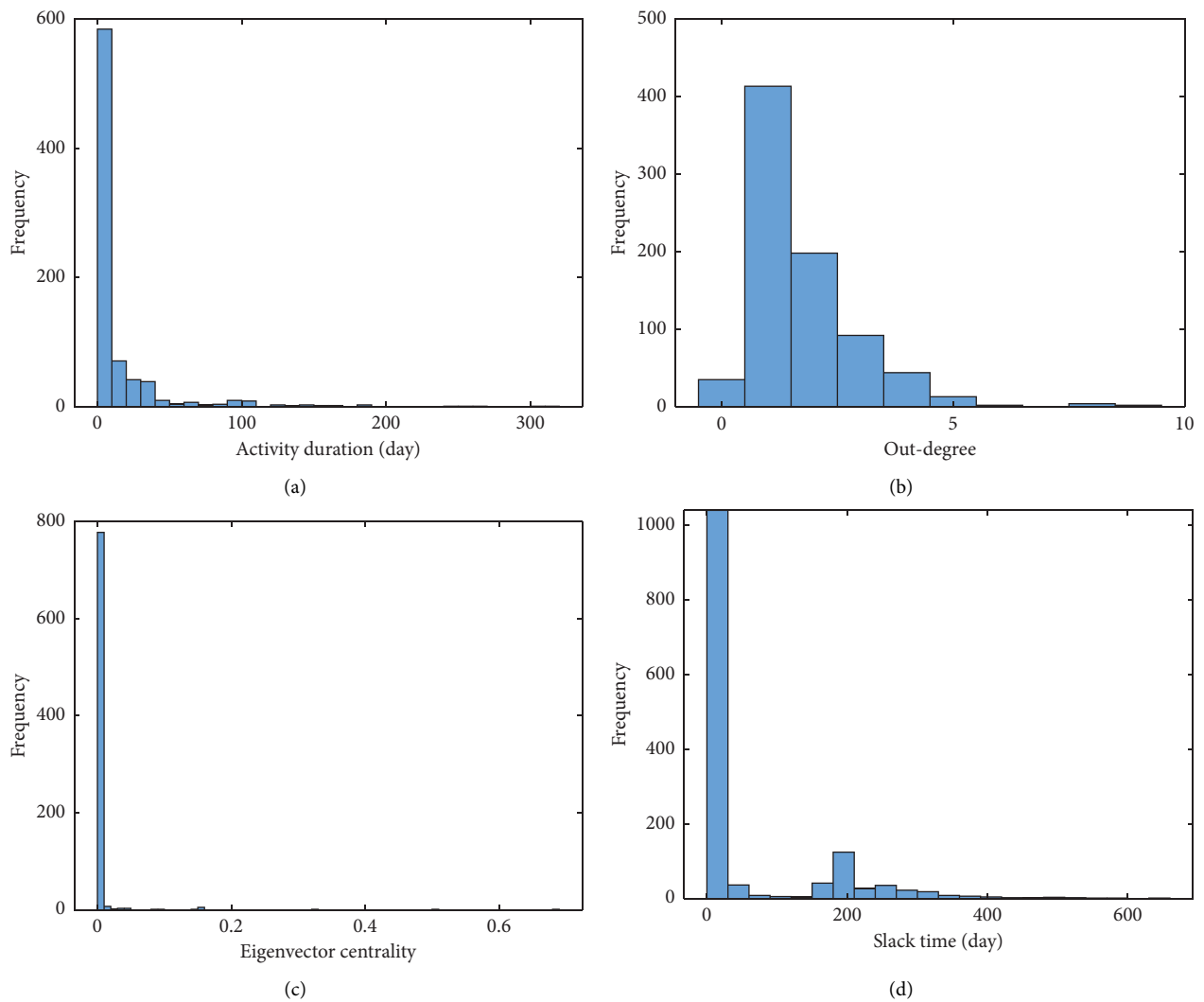


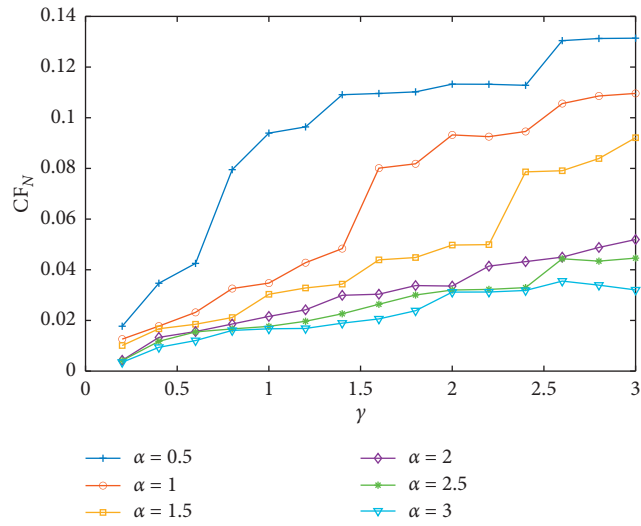
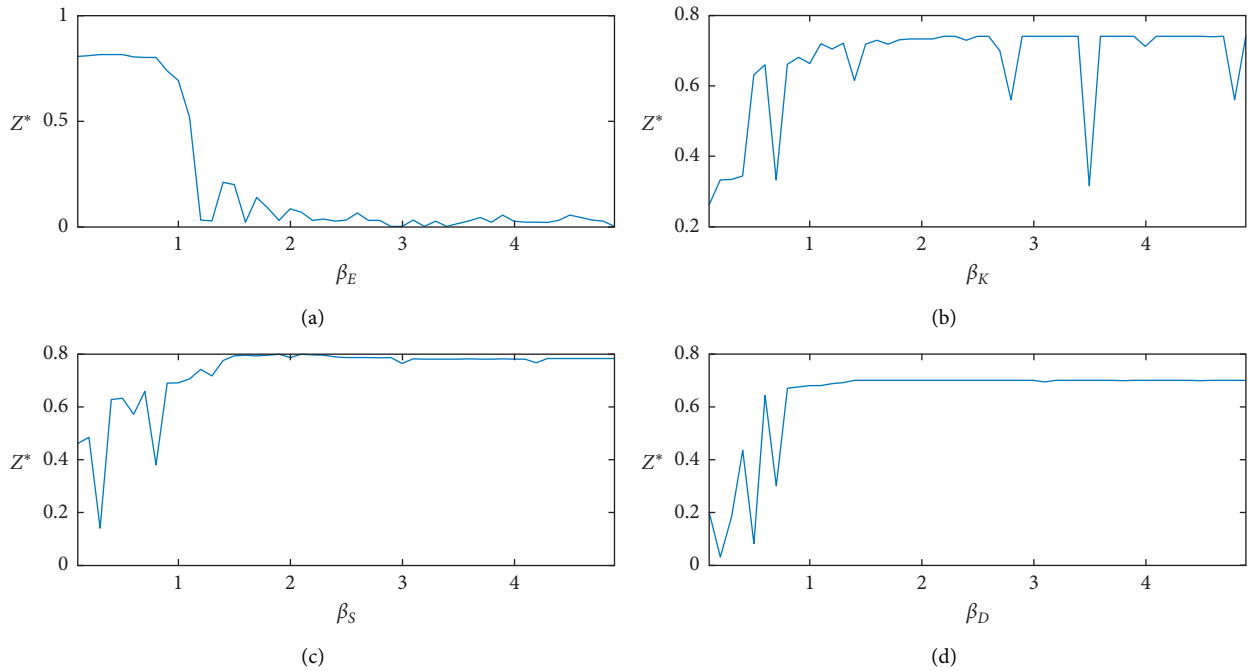
FIGURE 5: Data distribution: histogram of (a) duration, (b) out-degree, (c) eigenvector centrality, and (d) slack time.

relationship between the node capacity and β_D . Furthermore, the figures show the occurrence of several outliers, such as $\beta_K = 7, 14, 27, 28$ in Figure 7(b), $\beta_S = 3, 8$ in

Figure 7(c), and $\beta_D = 2, 5, 7$ in Figure 7(d). Using β_K as an example, different nodes have different out-degrees, which allows β_K to have different impacts on each node. When

TABLE 2: Initial values of parameters.

Parameter	Description	Initial value
α	Capacity level	0.2
γ	Infection intensity	0.5
β_K	Influence of out-degree on risk resistance	1
β_D	Influence of duration on risk resistance	1
β_E	Influence of eigenvector centrality on infection rate	1
β_S	Influence of slack time on infection rate	1

FIGURE 6: Relationship between CF_N and γ for different α .FIGURE 7: Effects of β_E , β_K , β_S , and β_D ($\alpha = 0.2$, $\gamma = 0.5$). Relation between (a) Z^* and β_E , (b) Z^* and β_K , (c) Z^* and β_S , and (d) Z^* and β_D .

nodes whose out-degree changed slightly with β_K were in the pathways developed by risk propagation, the possibility of infection decreased.

Figure 8 shows that increasing parameter β_D led to values of CF_N^{ST} being higher than CF_N^{END} , demonstrating the effect that the activity duration had on resisting the end date

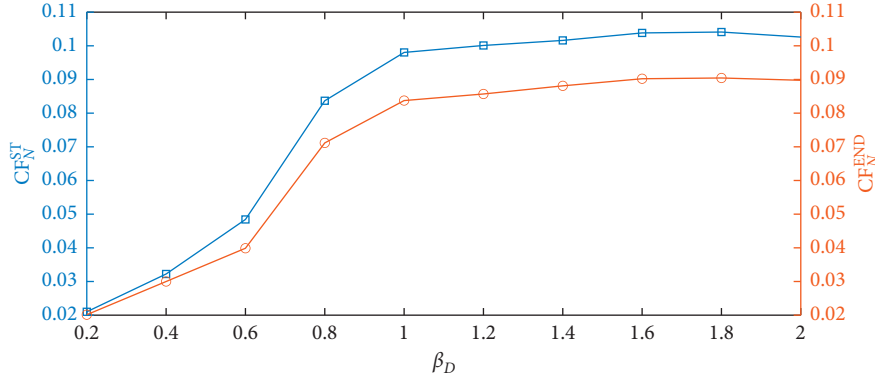


FIGURE 8: Effects of activity duration on end date change risk.

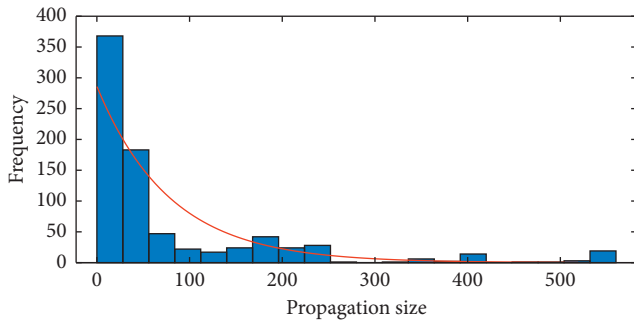


FIGURE 9: Distribution of propagation size.

change risk. When $\beta_D < 0.4$, the values of CF_N^{ST} and CF_N^{END} were close and low. When $\beta_D > 0.8$, the difference between CF_N^{ST} and CF_N^{END} reached a stable value.

Considering an environment defined by the parameters given in Table 2, each node i in the AON was purposely infected, and the size of each risk propagation was collected. The histogram of the propagation size with a fitted exponential distribution is shown in Figure 9. The size of the maximum propagation was 553. There were fewer large sizes and more small sizes.

Based on the above analysis, some important insights can be drawn for project managers. First, a single activity change can be sufficient to cause cascading changes in many downstream activities. Meanwhile, a larger number of activities have limited capacities to trigger a change propagation (Figure 9). Hence, it is vital for managers to identify critical activities and allocate resources to these activities to resist the change risk. The simulation model can help managers predict risk propagation and evaluate the importance of each activity. Second, with an increase in the risk threshold, the ability to resist the change risk can be improved. Managers can improve the capacity level of each node and allocate more resources to nodes with higher out-degrees using methods such as accelerating monitoring and feedback and preparing redundant resources for activities. However, the risk threshold is limited by the cost as well as the decrease in the marginal capacity (Figure 6). Third, managers can reduce the propagation by controlling the infection rate. The simulation results indicated that the slack time between activities and the eigenvector centrality is

correlated to the infection rate. Although adjusting the eigenvector centralities of nodes is difficult, managers can strengthen the monitoring of these nodes to prevent the infection. Furthermore, when making the project schedule, managers can consider allocating extra time to critical activities in case of schedule changes.

5. Conclusions

In this paper, a risk propagation model of schedule changes on an AON network was constructed based on the susceptible-infected (SI) model and the threshold model. A set of factors are considered to represent the risk threshold and infection rate, including the capacity level, node duration, node out-degree, eigenvector centrality of the node, infection intensity, and slack time. Transition rules are designed to determine the dynamics of the model. By simulating the risk propagation model, three conclusions are made: (1) The capacity level and infection intensity both influence the risk propagation, but both have limitations. At the same time, the convergence rate of the propagation is highly correlated to the capacity level. (2) The out-degree, slack time, and activity duration have negative impacts on the number of infected nodes, while the eigenvector centrality has a positive impact. (3) The number of start date change risks is greater than the number of end date change risks due to the impact of the activity duration on resisting the latter. Furthermore, the distribution of the number of infected nodes is similar to an exponential distribution, making it vital for the identification of critical nodes.

This paper introduces the framework of a risk propagation model to the field of project management. The framework could also be applied to research in other areas of risk management, such as safety or quality risk. First, networks are constructed with nodes representing resources and edges representing the impact between nodes. Second, risks are identified, and the dynamics of the risk propagation are designed. Third, simulations are conducted to evaluate the impacts of factors.

To overcome the limitations in this work, the following aspects should be further explored in future work:

- (1) The impact of the extent of a schedule change is not considered in this paper, and the extent may play an

important role in risk propagation due to its influence on the infection rate. Therefore, the model can be refined to consider more characteristics of schedule changes.

- (2) This model only considers the susceptible (S) state, infected (I) state, and transition from S to I, and it ignores the effects of mitigation strategies and the transition from I to S. To make the model more realistic, simulations of the schedule risk propagation must be conducted in real time, and more states and mitigation strategies can be added to the simulation.
- (3) Construction projects are very complex, involving many different external risk factors. How to integrate these factors into the model and construct a comprehensive risk index system will also be considered in future work.

Data Availability

The data used to support the findings of this study are available from the corresponding author upon request.

Conflicts of Interest

The authors declare that there are no conflicts of interest regarding the publication of this paper.

Acknowledgments

This work was supported by the National Natural Science Foundation of China (Grant no. 71601047) and China Postdoctoral Science Foundation (Grant no. 2015M581706).

References

- [1] K. El-Rayes and A. Kandil, "Time-cost-quality trade-off analysis for highway construction," *Journal of Construction Engineering and Management*, vol. 131, no. 4, pp. 477–486, 2005.
- [2] Ö. Öztaş and A. Öztaş, "Construction project network evaluation with correlated schedule risk analysis model," *Journal of Construction Engineering and Management*, vol. 134, no. 1, pp. 49–63, 2008.
- [3] V. T. Luu, S.-Y. Kim, N. V. Tuan, and S. O. Ogunlana, "Quantifying schedule risk in construction projects using Bayesian belief networks," *International Journal of Project Management*, vol. 27, no. 1, pp. 39–50, 2009.
- [4] X. Xu, J. Wang, C. Z. Li, W. Huang, and N. Xia, "Schedule risk analysis of infrastructure projects: a hybrid dynamic approach," *Automation in Construction*, vol. 95, pp. 20–34, 2018.
- [5] M. Liu, G. Ballard, and W. Ibbs, "Work flow variation and labor productivity: case study," *Journal of Management in Engineering*, vol. 27, no. 4, pp. 236–242, 2011.
- [6] K. M. El-Gohary and R. F. Aziz, "Factors influencing construction labor productivity in Egypt," *Journal of Management in Engineering*, vol. 30, no. 1, pp. 1–9, 2014.
- [7] Construction Industry Institute (CII), *Project Control for Engineering, Publication 6-1, Cost/Schedule Control Task Force*, University of Texas, Austin, TX, USA., 1986.
- [8] C. Ellinas, N. Allan, C. Durugbo et al., "How robust is your project? From local failures to global catastrophes: a complex networks approach to project systemic risk," *PLoS One*, vol. 10, no. 11, Article ID e0142469, 2015.
- [9] L. Chen, Q. Lu, and X. Zhao, "Rethinking the construction schedule risk of infrastructure projects based on dialectical systems and network theory," *Journal of Management in Engineering*, vol. 36, no. 5, Article ID 04020066, 2020.
- [10] C. Z. Li, X. Xu, G. Q. Shen, C. Fan, X. Li, and J. Hong, "A model for simulating schedule risks in prefabrication housing production: a case study of six-day cycle assembly activities in Hong Kong," *Journal of Cleaner Production*, vol. 185, pp. 366–381, 2018.
- [11] W. Ibbs and L. D. Nguyen, "Schedule analysis under the effect of resource allocation," *Journal of Construction Engineering and Management*, vol. 133, no. 2, pp. 131–138, 2007.
- [12] J. B. H. Yap, H. Abdul-Rahman, and C. Wang, "Preventive mitigation of overruns with project communication management and continuous learning: PLS-SEM approach," *Journal of Construction Engineering and Management*, vol. 144, no. 5, Article ID 04018025, 2018.
- [13] O. B. Tokdemir, H. Erol, and I. Dikmen, "Delay risk assessment of repetitive construction projects using line-of-balance scheduling and Monte Carlo simulation," *Journal of Construction Engineering and Management*, vol. 145, no. 2, Article ID 04018132, 2019.
- [14] D. Nasir, B. McCabe, and L. Hartono, "Evaluating risk in construction-schedule model (ERIC-S): construction schedule risk model," *Journal of Construction Engineering and Management*, vol. 129, no. 5, pp. 518–527, 2003.
- [15] M. Hajdu, "Effects of the application of activity calendars on the distribution of project duration in PERT networks," *Automation in Construction*, vol. 35, pp. 397–404, 2013.
- [16] M. Vanhoucke, "Using activity sensitivity and network topology information to monitor project time performance," *Omega*, vol. 38, no. 5, pp. 359–370, 2010.
- [17] P. Ballesteros-Pérez, A. Cerezo-Narváez, M. Otero-Mateo et al., "Performance comparison of activity sensitivity metrics in schedule risk analysis," *Automation in Construction*, vol. 106, Article ID 102906, 2019.
- [18] J. Song, A. Martens, and M. Vanhoucke, "Using schedule risk analysis with resource constraints for project control," *European Journal of Operational Research*, vol. 288, no. 3, pp. 736–752, 2020.
- [19] M. V. Leduc, S. Poledna, and S. Thurner, "Systemic risk management in financial networks with credit default swaps," *Journal of Network Theory in Finance*, vol. 3, no. 3, pp. 19–30, 2017.
- [20] X. Guan and C. Chen, "General methodology for inferring failure-spreading dynamics in networks," *Proceedings of the National Academy of Sciences*, vol. 115, no. 35, pp. E8125–E8134, 2018.
- [21] C. Ellinas, "Modelling indirect interactions during failure spreading in a project activity network," *Scientific Report*, vol. 8, Article ID 4373, 2018.
- [22] N. Guo, P. Guo, H. Dong, J. Zhao, and Q. Han, "Modeling and analysis of cascading failures in projects: a complex network approach," *Computers & Industrial Engineering*, vol. 127, pp. 1–7, 2019.
- [23] R. Li, N. Yang, Y. Zhang et al., "Risk propagation and mitigation of design change for complex product development (CPD) projects based on multilayer network theory," *Computers & Industrial Engineering*, vol. 142, Article ID 106370, 2020.

- [24] A. M. del Rey, G. Hernández, A. B. Taberner et al., “Advanced malware propagation on random complex networks,” *Neurocomputing*, 2020, In press.
- [25] W. Ibbs, L. D. Nguyen, and S. Lee, “Quantified impacts of project change,” *Journal of Professional Issues in Engineering Education and Practice*, vol. 133, no. 1, pp. 45–52, 2007.
- [26] P. E. D. Love, G. D. Holt, L. Y. Shen, H. Li, and Z. Irani, “Using systems dynamics to better understand change and rework in construction project management systems,” *International Journal of Project Management*, vol. 20, no. 6, pp. 425–436, 2002.
- [27] M. Park and F. Peña-Mora, “Dynamic change management for construction: introducing the change cycle into model-based project management,” *System Dynamics Review*, vol. 19, no. 3, pp. 213–242, 2003.
- [28] R. Ansari, “Dynamic simulation model for project change-management policies: engineering project case,” *Journal of Construction Engineering and Management*, vol. 145, no. 7, Article ID 05019008, 2019.
- [29] Z. Wu, K. Yang, X. Lai et al., “A scientometric review of system dynamics applications in construction management research,” *Sustainability*, vol. 12, no. 18, Article ID 7474, 2020.
- [30] D. N. Ford and J. D. Sterman, “Dynamic modeling of product development processes,” *System Dynamics Review*, vol. 14, no. 1, pp. 31–68, 1998.
- [31] I. A. Motawa, C. J. Anumba, S. Lee, and F. Peña-Mora, “An integrated system for change management in construction,” *Automation in Construction*, vol. 16, no. 3, pp. 368–377, 2007.
- [32] Z. Y. Zhao, Q. L. Lv, J. Zuo, and G. Zillante, “Prediction system for change management in construction project,” *Journal of Construction Engineering and Management*, vol. 136, no. 6, pp. 659–669, 2010.
- [33] G. Heravi and M. H. Charkhakan, “Predicting change by evaluating the change implementation process in construction projects using event tree analysis,” *Journal of Management in Engineering*, vol. 31, no. 5, Article ID 04014081, 2015.
- [34] A. V. O. Oliveros and A. R. Fayek, “Fuzzy logic approach for activity delay analysis and schedule updating,” *Journal of Construction Engineering and Management*, vol. 131, no. 1, pp. 42–51, 2005.
- [35] K. Cho, T. Kim, and T. Hong, “Estimating a risk-integrated schedule delay for an office building renovation project by considering the project’s attributes,” *Journal of Management in Engineering*, vol. 36, no. 2, Article ID 04019040, 2020.
- [36] C. Ellinas, N. Allan, and A. Johansson, “Project systemic risk: application examples of a network model,” *International Journal of Production Economics*, vol. 182, pp. 50–62, 2016.
- [37] A. E. Motter and Y. Lai, “Cascade-based attacks project systemic risk: application examples of a network model,” *Physical Review E: Statistical, Nonlinear, and Soft Matter Physics*, vol. 66, no. 6, Article ID 065102, 2002.
- [38] A. Barabasi and M. Posfai, *Network Science*, Cambridge University Press, Cambridge, UK, 2016.
- [39] D. J. Watts, “A simple model of global cascades on random networks,” *Proceedings of the National Academy of Sciences*, vol. 99, no. 9, pp. 5766–5771, 2002.
- [40] R. Pastor-Satorras and A. Vespignani, “Epidemic spreading in scale-free networks,” *Physical Review Letters*, vol. 86, no. 14, pp. 3200–3203, 2000.
- [41] T. Chen, S. Wu, J. Yang, and G. Cong, “Risk propagation model and its simulation of emergency logistics network based on material reliability,” *International Journal of Environmental Research and Public Health*, vol. 16, no. 23, p. 4677, 2019.
- [42] Project Management Institute, *A Guide to the Project Management Body of Knowledge: PMBOK Guide*, Project Management Institute, Newtown Square, PA, USA, 2013.
- [43] G. S. Canright and K. Engø-Monsen, “Spreading on networks: a topographic view,” *Complexus*, vol. 3, no. 1–3, pp. 131–146, 2006.